

Theoretical Mechanistic Study of Nickel(0)/Lewis Acid Catalyzed Polyfluoroarylcyanation of Alkynes: Origin of Selectivity for C–CN Bond Activation

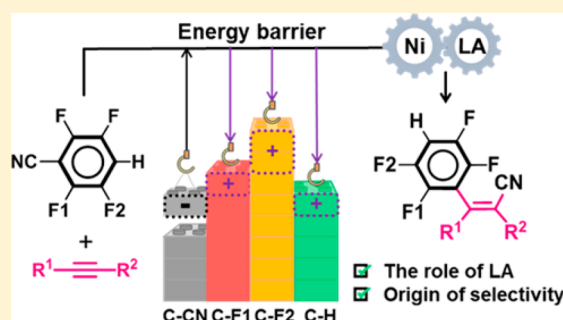
Hang Ren,^{†,§} Gui-Fang Du,^{†,§} Bo Zhu,[†] Guo-Chun Yang,^{†,‡} Li-Shuang Yao,[‡] Wei Guan,^{*,†,‡,‡} and Zhong-Min Su^{†,‡}

[†]Faculty of Chemistry, National & Local United Engineering Lab for Power Battery, Key Laboratory for UV-Emitting Materials and Technology of Ministry of Education, Northeast Normal University, Changchun 130024, P. R. China

[‡]State Key Laboratory of Applied Optics, Changchun Institute of Optics, Fine Mechanics and Physics, Chinese Academy of Sciences, Changchun 130033, P. R. China

S Supporting Information

ABSTRACT: The cooperative mechanism of Ni(0)/Lewis acid catalyzed carbocyanation of alkyne with 2,3,5,6-tetrafluorobenzonitrile was investigated using the DFT method. Our calculations indicate that the most feasible catalytic cycle consists of the oxidative addition of a C–CN bond to the Ni(0) center, alkyne insertion into the C(aryl)–Ni(II) bond, and reductive elimination. Notably, the Lewis acid (LA) interacting with the cyano nitrogen atom of the substrate can have a significant effect on activating the C–CN bond while suppressing C–H and C–F bond activations. The origin of lower C–CN activation barrier in the presence of LA can be attributed to the remarkably enhanced charge transfer (CT) amount from the Ni_{cat} 3d orbital to C–CN $\sigma^* + \pi^*$ antibonding molecular orbital and the little decrease of interaction energy between Ni-catalyst and substrate. In the C–F and C–H bond activations in the presence of LA, on the contrary, the significant decrease of interaction energy between Ni-catalyst and substrate and almost no change of charge transfer amounts are the origin of the larger bond activation barrier. Thus, LA is essential to make the C–CN bond weaker than other bonds, which agrees well with the experimental observation. Electronic processes as well as interaction energy analyses are discussed in detail.



INTRODUCTION

The selective activation of carbon–carbon (C–C) σ -bonds and subsequent functionalization into more valuable commodity and specialty chemicals have attracted more and more attention in synthesis and catalytic reactions.¹ In contrast to the more advanced field of C–H bond activation from the aspects of various transition metals (TMs),² however, the development of inert C–C bond activation by the TMs still remains inadequate.³ The situation should be attributed to their thermodynamic stability and kinetic inertia. In general, it is highly endothermic that a strong C–C bond activation (about 90 kcal/mol) leads to two comparatively weak metal–carbon bonds (30–60 kcal/mol).⁴ In addition, the C–C bond activation is hindered by low orbital overlap between the TM d_π orbital and the unoccupied C–C antibonding orbital because of their constrained directionality.^{1e} On many occasions, the more exposed C–H bonds will be preferred to be activated than C–C bonds. Thus, it is rather challenging to selectively activate C–C bonds in competition with surrounding C–H bonds of the substrate.⁵ Hence, to overcome these intrinsic difficulties, chemists have endeavored to devise various strategies, the relief of strain,⁶ achievement of

aromaticity,⁷ and irreversible elimination of functional groups,⁸ to achieve TM-mediated C–C bonds cleavage in recent years. However, the low selectivity is still the top challenge in this field. In this regard, a directing group, such as cyano,⁹ pyridyl,¹⁰ and quinolinyl¹¹ group, was usually employed to activate the C–C bond with high selectivity. In particular, the selective activation of C–CN bonds is of great significance, because the most extensively recognized industrial application is the DuPont's adiponitrile synthesis.¹² Meanwhile, nitrile groups are important blocks in organic synthesis that can be found in pharmaceuticals, pesticides, and organic materials.¹³

In a series of works, Jones and co-workers have made significant contributions in highly selective C–CN bond activation in the presence of C–H bonds.¹⁴ They concluded that C–H bond activation is favored kinetically, while C–CN bond activation is favored thermodynamically in the photochemical reaction catalyzed by rhodium.^{14d} Besides, they found σ -donating ligands^{14e} and nonpolar solvents^{14c} would be favorable for C–CN bond activation, but no reasonable

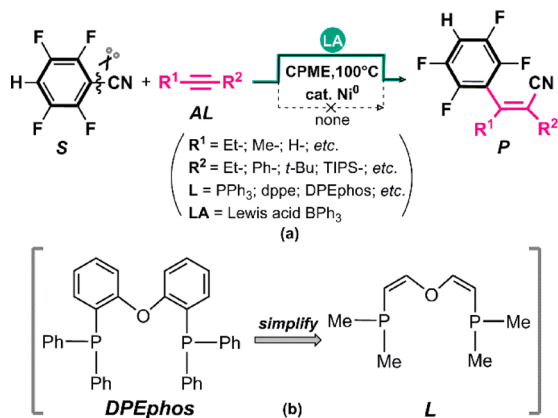
Received: May 19, 2018

Published: July 18, 2018

interpretation of high C–CN bond selectivity could be ascertained. Furthermore, the nitrile substrate scope of the selective C–CN bond activation by a TM catalyst was limited to the aryl and allyl cyanides. Thus, the further development of this field is restricted to a great extent and a new synthetic strategy is urgent to explore.

It is noteworthy that the cooperative catalysis strategy of the TM complex with the Lewis acid (LA) exhibits the highly powerful potential to activate the C–CN bonds in organic synthesis.¹⁵ A pioneering work that C–CN bond activation reaction of allyl cyanide was achieved using Ni(dippe)/BPh₃ cooperative catalysis has been reported by Jones and co-workers in 2004.¹⁶ It should be noted that their stoichiometric studies demonstrated that C–CN bond activation is faster than C–H bond in the presence of LA. Subsequently, Nakao and co-workers achieved the carbocyanation of inert alkynes and alkenes via C–CN bond cleavage in a selective manner without a directing moiety by Ni(0)/LA cooperative catalysis; meanwhile, the substrate tolerance is generally excellent.¹⁷ Matsubara and co-workers accomplished a Ni(0)/MAD cooperatively catalyzed decyanative [4 + 2] intermolecular cycloaddition reaction of *o*-arylcarboxybenzonitriles and alkynes involving the cleavage of both C–CN and C–O bonds.¹⁸ Recently, as shown in Scheme 1a, Nakao, Hiyama,

Scheme 1. (a) Experimentally Reported Ni(0)/LA-Catalyzed Polyfluoroarylcyanation of Alkynes. (b) The Exact Ligand (DPEphos) and the Model Ligand (L)



and co-workers successfully achieved polyfluoroarylcyanation of alkynes using Ni(0)/LA cooperative catalysis to produce a variety of fluorinated organic compounds, which would be accessible to liquid crystals and organic light-emitting diodes.¹⁹ It is notable that the C–CN bond is preferred to be activated by Ni(0)/LA over the C–H and C–F bonds and the yield of product is little or none in the absence of LA. A plausible mechanism involving oxidative addition of a C–CN bond, insertion of alkyne into the Ni–Ar_F bond, and reductive elimination was proposed. Nevertheless, the mechanistic details and the origin of selectivity for the C–CN bond activation remain ambiguous. In addition, those works mentioned above indicate that LA can significantly improve selectivity of C–CN bond activation, accelerate the reaction rate, or even trigger a difficult reaction. However, it is not easy to observe the reactive intermediates and clarify the reaction mechanisms experimentally. On the contrary, theoretical calculations have become useful protocols to provide meaningful information to understand the mechanisms and reaction

selectivity.²⁰ A recent theoretical investigation disclosed that the strong electron-withdrawing property of LA can not only strengthen the charge transfer from the metal to the C–CN $\sigma^* + \pi^*$ antibonding molecular orbital to promote the C–CN bond cleavage^{21a,b} but also accelerate alkyne migratory insertion.^{21c} However, the knowledge of cooperative catalysis of the TM/LA system remains inadequate, especially the origin of selective activation of different carbon-bond types. Such knowledge would provide meaningful information to understand the role of LA and further develop such TM/LA cooperative catalytic system for the inert C–C σ -bond activation reactions. Hence, it is of considerable importance to provide more thorough theoretical investigation of this cooperative catalysis of TM/LA.

In the present work, we theoretically investigated the full catalytic cycle of the Ni(0)/LA-catalyzed carbocyanation of alkyne with 2,3,5,6-tetrafluorobenzonitrile by density functional theory (DFT). Our purposes here are to disclose the mechanism of this catalytic reaction, clarify the origin of high selectivity of C–CN bond activation over C–H and C–F bonds, and elucidate the promoting effect of LA on this reaction.

COMPUTATIONAL DETAILS AND MODELS

According to the benchmark calculations in our previous study,^{21a,c,22} the M06 hybrid functional²³ was chosen here to perform geometry optimizations without symmetry constraints in the gas phase because of the little effect of solvation on the activation energy (Table S1, Supporting Information). Two kinds of basis set systems were employed here. In basis set system I (BSI), the LANL2DZ was employed for the Ni atom with effective core potentials (ECPs) for its core electrons.²⁴ The 6-31++G(d,p) and 6-31+G(d) were employed for H and F of polyfluoroarene, respectively. The 6-31G(d) basis set was employed for other main-group elements. The vibrational frequency was calculated for each stationary point to confirm whether it is a saddle point or minima. Intrinsic reaction coordinate (IRC)²⁵ calculation was conducted to ensure the transition state led to the correct reactant or product. Thermal corrections and entropy contributions of vibrational movements to the Gibbs energy change were evaluated at 373.15 K and 1 atm, in which the translational entropy was corrected to treat the standard state;²⁶ see page S2 in the Supporting Information. Furthermore, the Gibbs free energy in this work was calculated by adding the correction of Gibbs free energy in gas phase with the single-point energy in solution phase using a better basis set system (BSII).²⁷ In BSII, the Stuttgart–Dresden–Bonn (SDD) was employed for Ni with ECPs for the core electrons.²⁸ The 6-311++G(2d,2p) basis set was used to describe H of polyfluoroarene, whereas the 6-311+G(2d,p) basis set was employed for other elements. The solvent effect of diethyl ether was evaluated by the conductor-like polarizable continuum model (CPCM).²⁹ All calculations were carried out with the Gaussian 09 program.³⁰ The 3D molecular structures were generated using the CYLview program.³¹

In the present calculations, the polyfluoroarylcyanation of but-2-yne (AL) with 2,3,5,6-tetrafluorobenzonitrile (S) catalyzed by Ni(0)(L)/LA was chosen as the model reaction, where BPh₃ was adopted as LA. In addition, considering the computational efficiency, the exact ligand bis(2-diphenylphosphinophenyl) (DPEphos) was simplified to a model bidentate phosphorus-containing ligand (L = C₈H₁₆OP₂), as shown in Scheme 1b.

RESULTS AND DISCUSSION

For clarity, the following discussions are divided into two sections: the most favorable catalytic cycle of Ni(L)/LA-catalyzed carbocyanation of S with alkyne and the key role of LA.

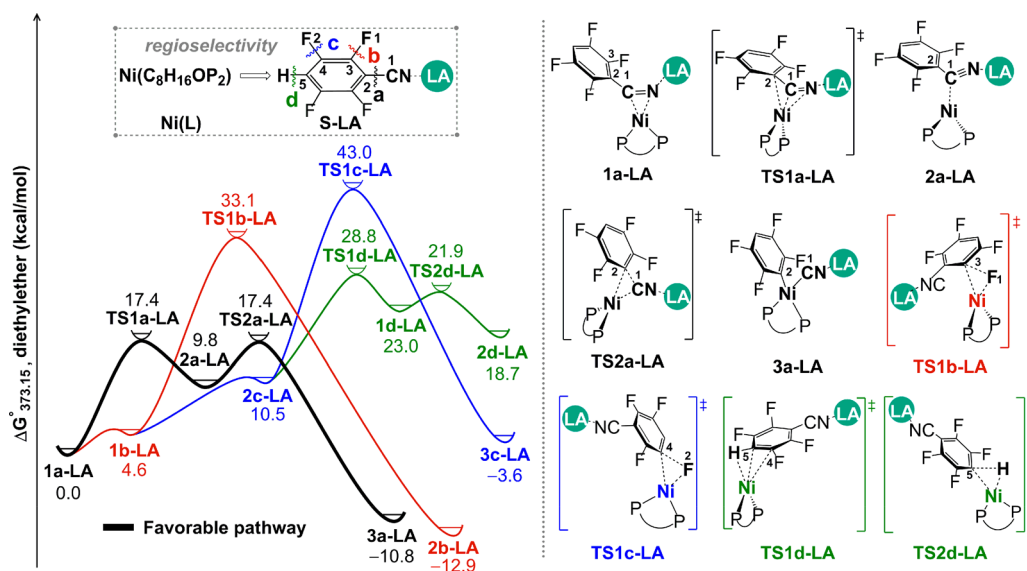


Figure 1. Energy profiles ($\Delta G^\circ_{373.15}$) for oxidative addition catalyzed by Ni(L)/LA.

The Most Favorable Catalytic Cycle. Oxidative Addition. As shown in Figure 1, the first key elementary step is oxidative addition of S-LA to the nickel(0) center in the present reaction. Note that there are four σ -bonds in S-LA (a–d; see the top inset in Figure 1); it is essential to investigate regioselectivity of the four σ -bonds which controls the product selectivity. Then, the regioselectivity was explored in detail from the kinetic point of view. First, we elucidated what the original precomplex is. Molecular electrostatic potential of S and various structure optimizations show that only the cyano nitrogen atom could interact with the electron-deficient LA (Figure S1, Supporting Information), which is in line with the experimental observation.¹⁹ Then, five kinds of adducts were considered, where Ni(L) coordinates with the C1 \equiv N triple bond (1a-LA), C2=C3 double bond (1b-LA), C3=C4 double bond (1c-LA), C4=C5 double bond (2c-LA), and C5–H single bond (1d-LA) in the phenyl ring of S-LA based on the lowest unoccupied molecular orbitals (LUMO) of S and S-LA (Figure S2 and Scheme S1, Supporting Information). Consequently, 1a-LA would be the initial precomplex, which is more stable than 1b-LA, 1c-LA, 2c-LA, and 1d-LA by about 4.6, 11.8, 10.5, and 23.0 kcal/mol, respectively. This is not surprising because the LUMO of S-LA delocalizes mostly over the C–CN moiety, thus indicating Ni(L) can prefer to coordinate with a C–CN bond (Table S2, Supporting Information). Subsequently, from 1a-LA, four kinds of transition states for bond activation (a–d) were located (Figure 1): (a) TS2a-LA for the C1–C2 bond activation, (b) TS1b-LA for the C3–F1 bond activation, (c) TS1c-LA for the C4–F2 bond activation, and (d) TS2d-LA for the C5–H bond activation. Furthermore, the triplet potential surface lies much higher than the singlet one on the basis of the Gibbs energy calculated on the potential energy surface (Table S3, Supporting Information).

As shown in Figure 1, prior to the oxidative addition, the Ni(0) center migrates to C1 of the aryl group from the C \equiv N bond to afford an intermediate 2a-LA through the transition state TS1a-LA, where the Ni–C1 bond is in a rocking motion with a Gibbs activation energy (ΔG°) of 17.4 kcal/mol. Starting from 2a-LA, the C–CN oxidative addition occurs via the concerted three-membered-ring transition state TS2a-LA,

in which the C1–C2 distance (1.52 Å) is longer than that in 2a-LA (1.48 Å), indicating that the cleavage of the C1–C2 bond is in progress. As a result, an intermediate 3a-LA can be obtained with a four-coordinated planar structure, in line with the general understanding of the d⁸ TM complex.³² In 3a-LA, the distance of C1–C2 elongates to 2.46 Å, indicating that the C1–C2 bond has been broken completely. The Gibbs activation energy and the Gibbs free energy change (ΔG°) of this process are 17.4 and –10.8 kcal/mol relative to 1a-LA, respectively (black line, Figure 1).

Alternatively, 1a-LA can isomerize to 1b-LA via migration of the Ni(0) center to the C2=C3 bond of the aryl group with slightly ΔG° of 4.6 kcal/mol; the similar migration process has been reported by Jones.³³ From 1b-LA, the C3–F1 bond can be activated via a similar three-membered-ring transition state TS1b-LA to afford 2b-LA with a larger ΔG° value of 33.1 kcal/mol and a ΔG° value of –12.9 kcal/mol (red line, Figure 1). In the C4–F2 bond activation, 1b-LA first isomerizes to complex 2c-LA via migration of the Ni(0) center to the C4=C5 bond of the aryl group. This isomerization is endothermic by 5.9 kcal/mol. The following cleavage of the C4–F2 bond occurs through rather high-energy transition state TS1c-LA to afford an intermediate 3c-LA ($\Delta G^\circ = 43.0$ kcal/mol and $\Delta G^\circ = -3.6$ kcal/mol relative to 1a-LA, blue line, Figure 1). The free energy profile of C5–H bond activation is shown in the green line of Figure 1; the formation of corresponding product 2d-LA occurs through Ni migration and then C–H oxidation addition steps. TS1d-LA and TS2d-LA are the transition states for these two steps with the ΔG° values of 28.8 and 21.9 kcal/mol, respectively. Overall, the energy barrier of C–CN bond activation is the smallest, which is in agreement with experiment observation that only the C–CN bond was selectively activated by Ni(L)/LA synergistic catalytic systems. In addition, we have reproduced successfully the competition reaction between S and benzonitrile catalyzed by Ni(L)/LA in the reaction mixture (Figure S3, Supporting Information).¹⁹

Alkyne Insertion and Reductive Elimination. The next process is alkyne insertion, in which AL first coordinates with the Ni(II) center of 3a-LA to provide an intermediate 4a-LA with a ΔG° value of 8.2 kcal/mol, as shown in Figure 2 and Figure S4 (Supporting Information). Consequently, one “arm”

Furthermore, in order to verify the rationality of the model simplification, we employed the exact Ni(DPEphos)/BPh₃ cocatalysts to evaluate the key selectivity-determining and rate-determining transition states (Table S4, Supporting Information).

The Role of the Lewis Acid. In the present reaction, LA could significantly promote the selective C–CN bond activation. To reveal the origin, we have fully evaluated the oxidative additions of each bond in the absence of LA (Figure S5, Supporting Information). Interestingly, the regioselectivity of the oxidative additions by Ni(L)/LA is found to be different from that by Ni(L), as shown in Figure 4. In the former case,

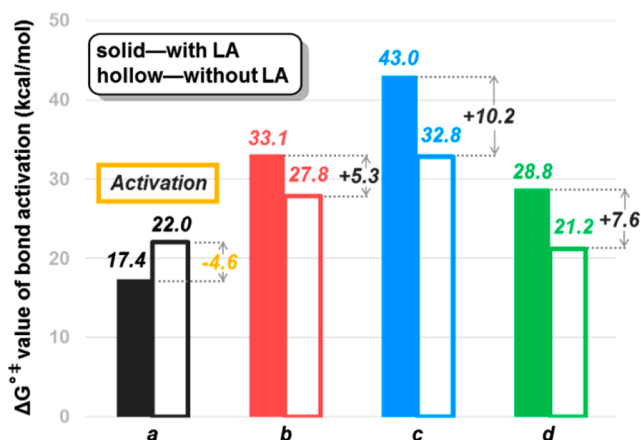


Figure 4. Gibbs activation energy for oxidative addition with/without LA.

the C–CN bond is cleaved with the smallest ΔG^{\ddagger} value (17.4 kcal/mol) in competition with the C–F and C–H bonds. In the latter case, the C–H bond activation is slightly lower than that of the C–CN bond by 0.8 kcal/mol in the absence of LA with Ni(L) catalyst. Using the exact DPEphos ligand, the energy barrier gap between C–CN and C–H activation increases to 2.1 kcal/mol (Figure S6). Thus, the C–H bond cleavage would be favorable than the C–CN bond in the absence of LA in terms of kinetics. In addition, the C–H bond activation process without LA is highly endothermic by 11.7 kcal/mol to afford an active Ni(II) hydride intermediate **2d**, which might hinder the expected alkyne insertion from stable **3a** and lead to no desired product by C–CN bond activation.³⁴ By contrast, it can be seen that the presence of LA can reduce the energy barrier of C–CN bond activation, whereas it enlarges that of C–F and C–H bond activations. In other words, LA can promote C–CN bond activation and meanwhile suppress C–H and C–F bond activations to selectively achieve the present reaction.

It is of considerable importance to provide a clear explanation for this interesting consequence. First, we evaluated the bond dissociation energy (BDE, in kcal/mol) of substrates **S** and **S-LA** from the perspective of thermodynamics. It can be determined that the BDE changes in the order a (136.2) > b (125.8) \approx c (125.2) > d (122.5) for **S** and b (125.8) \approx c (125.0) > d (122.8) > a (112.7) for **S-LA**. It seems that one LA interacting with the cyano nitrogen atom of **S** significantly weakens the C–CN bond (a).

Previous studies indicate that the substantial charge transfer (CT) from the $3d_{\pi}$ orbital of Ni(0) to the low-lying empty $\sigma^* + \pi^*$ antibonding orbital of the substrate promotes the bond

activation.^{21a,b} In this regard, we carried out the charge decomposition analysis (CDA) for bond activation (a–d) with Multiwfn3.3.8.³⁵ Corresponding TSs with and without LA are divided into two fragments as **S/S-LA** and Ni(L) moieties, respectively. For the C–CN bond (a) activation, the total CT from the Ni 3d to the $\sigma^* + \pi^*$ C–CN orbital in TS1a and TS2a is 0.2093e, while that is 0.6349e in TS1a-LA and TS2a-LA, as shown in Figure 5 (see Figure S7 in the Supporting

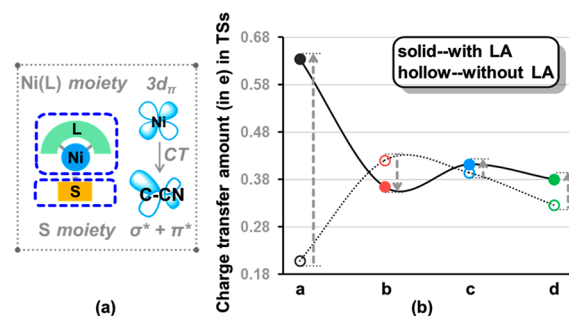


Figure 5. (a) Schematic picture of the MO of two moieties. (b) The amount of charge transfer in oxidative addition process with/without LA.

Information for more details). The changes of natural population analysis (NPA) are consistent with the CT discussed above (Figure S8, Supporting Information). Thus, the strong electron-withdrawing property of LA considerably stabilizes the unoccupied $\sigma^* + \pi^*$ C–CN antibonding orbital, accordingly enlarges such CT, and finally accelerates the C–CN bond activation.

By contrast, the similar CT in the other bond (b, c, and d) activations remains almost no change with and without LA. These CT results seem that LA has a great impact on the C–CN bond activation rather than the C–F and C–H bond activations. But is this the only origin for selective C–CN bond activation?

We first employed the activation strain model³⁶ to analyze the LA effect. As shown in Table 1, the energies of selected key

Table 1. Table 1. Distortion/Interaction Analysis (in kcal/mol) of Selected TSs Involving Various Bond Activations

	TS2a	TS1b	TS1c	TS1d
ΔE_{int}	31.7	20.4	24.1	45.4
ΔE_{dist}	−10.8	7.2	11.2	−23.3
ΔE^{\ddagger}	20.9	27.6	35.3	22.1
	TS2a-LA	TS1b-LA	TS1c-LA	TS1d-LA
ΔE_{int}	37.9	47.8	53.9	73.6
ΔE_{dist}	−18.3	−13.5	−6.4	−39.7
ΔE^{\ddagger}	19.6	34.3	47.5	33.9

TSs (TS2a, TS1b, TS1c, TS1d, TS2a-LA, TS1b-LA, TS1c-LA, TS1d-LA) have been divided into two parts: one is the distortion energy (ΔE_{dist}); the other is the interaction energy (ΔE_{int}). Note that the interaction terms are too large in original precomplex **1a** and **1a-LA**, so ΔE_{int} becomes positive in the corresponding TSs. Despite that there are some changes in ΔE_{dist} values, the ΔE_{int} plays a dominant role. Thus, the following discussions mainly focused on the ΔE_{int} between **S/S-LA** and Ni(L) moieties. The ΔE_{int} of TS2a, TS1b, TS1c, and TS1d relative to **1a** are 31.7, 20.4, 24.1 and 45.4, respectively, while those of TS2a-LA, TS1b-LA, TS1c-LA, and

TS1d-LA relative to 1a-LA are 37.9, 47.8, 53.9, and 73.6, respectively. It can be suggested from the more positive ΔE_{int} values that the LA has a stronger stabilizing effect on the precomplex 1a compared with the corresponding transition states of the oxidative additions. In this regard, the generation of the stable precomplex (1a-LA) would increase the ΔG^{\ddagger} values of the oxidative additions and accordingly inhibit the corresponding bond activations. As shown in Figure 6,

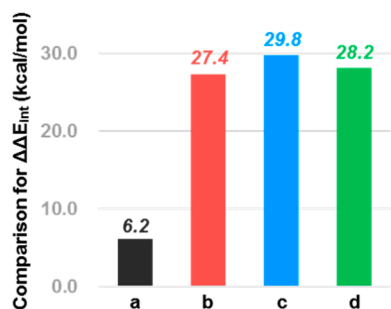


Figure 6. Interaction energy changes ($\Delta\Delta E_{\text{int}}$) of various TSs.

however, LA changes the order of the relative sequence of ΔE_{int} values because of the little decrease of interaction energy between Ni-catalyst and substrate ($\Delta\Delta E_{\text{int}}$ values). In the absence of LA, ΔE_{int} value of TS1b is the smallest, whereas that of TS2a-LA becomes the smallest one. In a word, the present selective C–CN bond activation can be responsible by both the smaller increased ΔE_{int} between substrate and catalyst and the larger CT from the Ni 3d to the $\sigma^* + \pi^*$ C–CN orbital.

CONCLUSIONS

Ni(0)/LA-catalyzed polyfluoroarylcyanation of alkynes was theoretically investigated with the DFT method. The overall catalytic cycle consists of three elementary steps: oxidative addition of a C–CN bond to the Ni(0) center, alkyne insertion into the Ni–C(aryl) bond, and reductive elimination. Alkyne insertion is the rate-determining step with the free energy barrier of 19.6 kcal/mol, which can be overcome under experimental conditions (100 °C).

The interesting regioselectivity in oxidative addition and the role of Lewis acid have also been studied. On one hand, LA enhances the charge transfer amount from the Ni(L) 3d_π orbital to the unoccupied $\sigma^* + \pi^*$ C–CN antibonding orbital, whereas it has no effect on C–H and C–F bonds. On the other hand, in the presence of LA, the generation of a more stable precomplex (1a-LA) inhibits the corresponding bond activations. The considerably large interaction energy decrease between Ni-catalyst and substrate in C–F and C–H bond activations is the origin of the larger bond activation barrier. It should be pointed out that the larger charge transfer amount and little interaction energy decrease make C–CN bond activation easier. The calculated result can match well with the experimental observation that the presence of LA plays a positive role in accelerating the reactions.

Such conclusions shed new light for understanding the selectivity of C–CN bond activation and would provide inspiration for experimental chemists to further design TMs/LA synergistic catalytic systems.

ASSOCIATED CONTENT

Supporting Information

The Supporting Information is available free of charge on the ACS Publications website at DOI: 10.1021/acs.organo-
met.8b00338.

Correction of translational entropy, Scheme S1, Figures S1–S8, Tables S1–S4 (PDF)

Cartesian coordinates of optimized structures (MOL)

AUTHOR INFORMATION

Corresponding Author

*E-mail: guanw580@nenu.edu.cn.

ORCID

Guo-Chun Yang: 0000-0003-3083-472X

Wei Guan: 0000-0001-7000-0274

Zhong-Min Su: 0000-0002-3342-1966

Author Contributions

[§]These authors contributed equally.

Notes

The authors declare no competing financial interest.

ACKNOWLEDGMENTS

This work has been financially supported by the NSFC (21773025, 21403033, and 61775212), the Fundamental Research Funds for the Central Universities, Open Project of Key Laboratory for UV-Emitting Materials and Technology of Ministry of Education (130028697), Jilin Provincial Education Department, and the State Key Laboratory of applied optics. We acknowledge the National Supercomputing Center in Shenzhen for providing the computational resources.

REFERENCES

- (1) (a) Murakami, M.; Matsuda, T. Metal-Catalysed Cleavage of Carbon-Carbon Bonds. *Chem. Commun.* **2011**, 47 (4), 1100–1105. (b) Chen, F.; Wang, T.; Jiao, N. Recent Advances in Transition-Metal-Catalyzed Functionalization of Unstrained Carbon-Carbon Bonds. *Chem. Rev.* **2014**, 114 (17), 8613–8661. (c) Souillart, L.; Cramer, N. Catalytic C–C Bond Activations via Oxidative Addition to Transition Metals. *Chem. Rev.* **2015**, 115 (17), 9410–9464. (d) Murakami, M.; Ishida, N. Potential of Metal-Catalyzed C–C Single Bond Cleavage for Organic Synthesis. *J. Am. Chem. Soc.* **2016**, 138 (42), 13759–13769. (e) Chen, P.-h.; Billett, B. A.; Tsukamoto, T.; Dong, G. Cut and Sew Transformations via Transition-Metal-Catalyzed Carbon-Carbon Bond Activation. *ACS Catal.* **2017**, 7 (2), 1340–1360.
- (2) (a) Shilov, A. E.; Shul'pin, G. B. Activation of C–H Bonds by Metal Complexes. *Chem. Rev.* **1997**, 97 (8), 2879–2932. (b) Dyker, G. Transition Metal Catalyzed Coupling Reactions under C–H Activation. *Angew. Chem., Int. Ed.* **1999**, 38 (12), 1698–1712. (c) Ritleng, V.; Sirlin, C.; Pfeffer, M. Ru-, Rh-, and Pd-Catalyzed C–C Bond Formation Involving C–H Activation and Addition on Unsaturated Substrates: Reactions and Mechanistic Aspects. *Chem. Rev.* **2002**, 102 (5), 1731–1770. (d) Godula, K.; Sames, D. C–H Bond Functionalization in Complex Organic Synthesis. *Science* **2006**, 312 (5770), 67. (e) Giri, R.; Shi, B.-F.; Engle, K. M.; Maugel, N.; Yu, J.-Q. Transition Metal-Catalyzed C–H Activation Reactions: Diastereoselectivity and Enantioselectivity. *Chem. Soc. Rev.* **2009**, 38 (11), 3242–3272. (f) Jazzar, R.; Hitce, J.; Renaudat, A.; Sofack-Kreutzer, J.; Baudoin, O. Functionalization of Organic Molecules by Transition-Metal-Catalyzed C(sp³)–H Activation. *Chem. - Eur. J.* **2010**, 16 (9), 2654–2672. (g) Wencel-Delord, J.; Droge, T.; Liu, F.; Glorius, F. Towards Mild Metal-Catalyzed C–H Bond Activation. *Chem. Soc. Rev.* **2011**, 40 (9), 4740–4761. (h) Chen, D. Y. K.; Youn, S. W. C–H Activation: A Complementary Tool in the Total Synthesis of

- Complex Natural Products. *Chem. - Eur. J.* **2012**, *18* (31), 9452–9474. (i) Luo, G.; Luo, Y.; Qu, J.; Hou, Z. Mechanistic Investigation on Scandium-Catalyzed C-H Addition of Pyridines to Olefins. *Organometallics* **2012**, *31* (10), 3930–3937. (j) Wencel-Delord, J.; Colobert, F. Asymmetric C(sp²)-H Activation. *Chem. - Eur. J.* **2013**, *19* (42), 14010–14017.
- (3) (a) Nájera, C.; Sansano, J. M. Asymmetric Intramolecular Carbocyanation of Alkenes by C-C Bond Activation. *Angew. Chem., Int. Ed.* **2009**, *48* (14), 2452–2456. (b) Ruhland, K. Transition-Metal-Mediated Cleavage and Activation of C-C Single Bonds. *Eur. J. Org. Chem.* **2012**, *2012* (14), 2683–2706. (c) Wen, Q.; Lu, P.; Wang, Y. Recent Advances in Transition-Metal-Catalyzed C-CN Bond Activations. *RSC Adv.* **2014**, *4* (88), 47806–47826. (d) Zhang, S.-L.; Huang, L.; Bie, W.-F. Mechanism for Activation of the C-CN Bond of Nitriles by a Cationic CpRh^{III}-Silyl Complex: A Systematic DFT Study. *Organometallics* **2014**, *33* (12), 3030–3039. (e) Kang, X.; Luo, G.; Luo, L.; Hu, S.; Luo, Y.; Hou, Z. Mechanistic Insights into Ring Cleavage and Contraction of Benzene over a Titanium Hydride Cluster. *J. Am. Chem. Soc.* **2016**, *138* (36), 11550–11559.
- (4) Halpern, J. Determination and Significance of Transition Metal-Alkyl Bond Dissociation Energies. *Acc. Chem. Res.* **1982**, *15* (8), 238–244.
- (5) (a) Rybtchinski, B.; Milstein, D. Metal Insertion into C-C Bonds in Solution. *Angew. Chem., Int. Ed.* **1999**, *38* (7), 870–883. (b) Rybtchinski, B.; Oevers, S.; Montag, M.; Vigalok, A.; Rozenberg, H.; Martin, J. M. L.; Milstein, D. Comparison of Steric and Electronic Requirements for C-C and C-H Bond Activation. Chelating vs Nonchelating Case. *J. Am. Chem. Soc.* **2001**, *123* (37), 9064–9077. (c) Miscione, G. P.; Bottoni, A. C-CN vs C-H Activation: Actual Mechanism of the Reaction between [(dippe)-PtH]₂ and Benzonitrile Evidenced by a DFT Computational Investigation. *Organometallics* **2014**, *33* (16), 4173–4182.
- (6) (a) Kulinkovich, O. G. The Chemistry of Cyclopropanols. *Chem. Rev.* **2003**, *103* (7), 2597–2632. (b) Rubin, M.; Rubina, M.; Gevorgyan, V. Transition Metal Chemistry of Cyclopropanes and Cyclopropanes. *Chem. Rev.* **2007**, *107* (7), 3117–3179. (c) Carson, C. A.; Kerr, M. A. Heterocycles from Cyclopropanes: Applications in Natural Product Synthesis. *Chem. Soc. Rev.* **2009**, *38* (11), 3051–3060. (d) Seiser, T.; Saget, T.; Tran, D. N.; Cramer, N. Cyclobutanes in Catalysis. *Angew. Chem., Int. Ed.* **2011**, *50* (34), 7740–7752. (e) Masarwa, A.; Didier, D.; Zabrodski, T.; Schinkel, M.; Ackermann, L.; Marek, I. Merging Allylic Carbon-Hydrogen and Selective Carbon-Carbon Bond Activation. *Nature* **2014**, *505*, 199. (f) Souillart, L.; Parker, E.; Cramer, N. Highly Enantioselective Rhodium(I)-Catalyzed Activation of Enantiotopic Cyclobutanone C-C Bonds. *Angew. Chem., Int. Ed.* **2014**, *53* (11), 3001–3005. (g) Chen, P. h.; Xu, T.; Dong, G. Divergent Syntheses of Fused β -Naphthol and Indene Scaffolds by Rhodium-Catalyzed Direct and Decarbonylative Alkyne-Benzocyclobutenone Couplings. *Angew. Chem., Int. Ed.* **2014**, *53* (6), 1674–1678.
- (7) (a) Fisher, E. L.; Lambert, T. H. Leaving Group Potential of a Substituted Cyclopentadienyl Anion Toward Oxidative Addition. *Org. Lett.* **2009**, *11* (18), 4108–4110. (b) Youn, S. W.; Kim, B. S.; Jagdale, A. R. Pd-Catalyzed Sequential C-C Bond Formation and Cleavage: Evidence for an Unexpected Generation of Arylpalladium(II) Species. *J. Am. Chem. Soc.* **2012**, *134* (28), 11308–11311.
- (8) (a) Goßen, L. J.; Deng, G.; Levy, L. M. Synthesis of Biaryls via Catalytic Decarboxylative Coupling. *Science* **2006**, *313* (5787), 662. (b) Tobisu, M.; Kita, Y.; Ano, Y.; Chatani, N. Rhodium-Catalyzed Silylation and Intramolecular Arylation of Nitriles via the Silicon-Assisted Cleavage of Carbon-Cyano Bonds. *J. Am. Chem. Soc.* **2008**, *130* (47), 15982–15989. (c) Cicchillo, R. M.; Zhang, H.; Blodgett, J. A. V.; Whitteck, J. T.; Li, G.; Nair, S. K.; van der Donk, W. A.; Metcalf, W. W. An Unusual Carbon-Carbon Bond Cleavage Reaction During Phosphinothricin Biosynthesis. *Nature* **2009**, *459*, 871. (d) He, C.; Guo, S.; Huang, L.; Lei, A. Copper Catalyzed Arylation/C-C Bond Activation: An Approach toward α -Aryl Ketones. *J. Am. Chem. Soc.* **2010**, *132* (24), 8273–8275. (e) Amaike, K.; Muto, K.; Yamaguchi, J.; Itami, K. Decarbonylative C-H Coupling of Azoles and Aryl Esters: Unprecedented Nickel Catalysis and Application to the Synthesis of Muscoride A. *J. Am. Chem. Soc.* **2012**, *134* (33), 13573–13576. (f) Tobisu, M.; Kinuta, H.; Kita, Y.; Rémond, E.; Chatani, N. Rhodium(I)-Catalyzed Borylation of Nitriles through the Cleavage of Carbon-Cyano Bonds. *J. Am. Chem. Soc.* **2012**, *134* (1), 115–118.
- (9) Jin, J.; Wen, Q.; Lu, P.; Wang, Y. Copper-Catalyzed Cyanation of Arenes Using Benzyl Nitrile as a Cyanide Anion Surrogate. *Chem. Commun.* **2012**, *48* (79), 9933–9935.
- (10) (a) Chatani, N.; Ie, Y.; Kakiuchi, F.; Murai, S. Ru₃(CO)₁₂-Catalyzed Decarbonylative Cleavage of a C-C Bond of Alkyl Phenyl Ketones. *J. Am. Chem. Soc.* **1999**, *121* (37), 8645–8646. (b) Niwa, T.; Yorimitsu, H.; Oshima, K. Palladium-Catalyzed 2-Pyridylmethyl Transfer from 2- (2-Pyridyl)ethanol Derivatives to Organic Halides by Chelation-Assisted Cleavage of Unstrained C-C Bonds. *Angew. Chem., Int. Ed.* **2007**, *46* (15), 2643–2645.
- (11) Dreis, A. M.; Douglas, C. J. Catalytic Carbon-Carbon σ Bond Activation: An Intramolecular Carbo-Acylation Reaction with Acylquinolines. *J. Am. Chem. Soc.* **2009**, *131* (2), 412–413.
- (12) Parshall, G. W.; Ittel, S. D. In *Homogeneous Catalysis: the Applications and Chemistry of Catalysis by Soluble Transition Metal Complexes*; Wiley: New York, 1992; pp 42–50.
- (13) Nakao, Y. In *C-C Bond Activation*; Springer: Heidelberg, 2014; pp 33–58.
- (14) (a) Garcia, J. J.; Brunkan, N. M.; Jones, W. D. Cleavage of Carbon-Carbon Bonds in Aromatic Nitriles Using Nickel(0). *J. Am. Chem. Soc.* **2002**, *124* (32), 9547–9555. (b) Ateşin, T. A.; Li, T.; Lachaize, S.; Brennessel, W. W.; García, J. J.; Jones, W. D. Experimental and Theoretical Examination of C-CN and C-H Bond Activations of Acetonitrile Using Zerovalent Nickel. *J. Am. Chem. Soc.* **2007**, *129* (24), 7562–7569. (c) Swartz, B. D.; Reinartz, N. M.; Brennessel, W. W.; García, J. J.; Jones, W. D. Solvent Effects and Activation Parameters in the Competitive Cleavage of C-CN and C-H Bonds in 2-Methyl-3-Butenenitrile Using [(dippe)NiH]₂. *J. Am. Chem. Soc.* **2008**, *130* (26), 8548–8554. (d) Evans, M. E.; Li, T.; Jones, W. D. C-H vs C-C Bond Activation of Acetonitrile and Benzonitrile via Oxidative Addition: Rhodium vs Nickel and Cp* vs Tp' (Tp' = Hydrotris(3,5-dimethylpyrazol-1-yl)borate, Cp* = η^5 -Pentamethylcyclopentadienyl). *J. Am. Chem. Soc.* **2010**, *132* (45), 16278–16284. (e) Evans, M. E.; Jones, W. D. Controlling the Selectivity for C-H and C-CN Bond Activation at Rhodium: A DFT Examination of Ligand Effects. *Organometallics* **2011**, *30* (12), 3371–3377. (f) Swartz, B. D.; Brennessel, W. W.; Jones, W. D. C-CN vs C-H Cleavage of Benzonitrile Using [(dippe)PtH]₂. *Organometallics* **2011**, *30* (6), 1523–1529.
- (15) (a) Wang, C.; Xi, Z. Co-Operative Effect of Lewis Acids with Transition Metals for Organic Synthesis. *Chem. Soc. Rev.* **2007**, *36* (9), 1395–1406. (b) Sakaki, S. Theoretical and Computational Study of a Complex System Consisting of Transition Metal Element(s): How to Understand and Predict Its Geometry, Bonding Nature, Molecular Property, and Reaction Behavior. *Bull. Chem. Soc. Jpn.* **2015**, *88* (7), 889–938. (c) Guan, W.; Zeng, G.; Kameo, H.; Nakao, Y.; Sakaki, S. Cooperative Catalysis of Combined Systems of Transition-Metal Complexes with Lewis Acids: Theoretical Understanding. *Chem. Rec.* **2016**, *16* (5), 2405–2425.
- (16) Brunkan, N. M.; Brestensky, D. M.; Jones, W. D. Kinetics, Thermodynamics, and Effect of BPh₃ on Competitive C-C and C-H Bond Activation Reactions in the Interconversion of Allyl Cyanide by [Ni(dippe)]. *J. Am. Chem. Soc.* **2004**, *126* (11), 3627–3641.
- (17) (a) Nakao, Y.; Yada, A.; Ebata, S.; Hiyama, T. A Dramatic Effect of Lewis-Acid Catalysts on Nickel-Catalyzed Carbocyanation of Alkynes. *J. Am. Chem. Soc.* **2007**, *129* (9), 2428–2429. (b) Nakao, Y.; Ebata, S.; Yada, A.; Hiyama, T.; Ikawa, M.; Ogoshi, S. Intramolecular Arylcyanation of Alkenes Catalyzed by Nickel/AlMe₂Cl. *J. Am. Chem. Soc.* **2008**, *130* (39), 12874–12875. (c) Hirata, Y.; Yada, A.; Morita, E.; Nakao, Y.; Hiyama, T.; Ohashi, M.; Ogoshi, S. Nickel/Lewis Acid-Catalyzed Cyanoesterification and Cyanocarbamoylation of Alkynes. *J. Am. Chem. Soc.* **2010**, *132* (29), 10070–10077. (d) Nakao, Y.; Yada,

- A.; Hiyama, T. Heteroatom-Directed Alkylcyanation of Alkynes. *J. Am. Chem. Soc.* **2010**, *132* (29), 10024–10026.
- (18) Methylaluminum bis(2,6-di-*tert*-butyl-4-methylphenoxide) is abbreviated as MAD. Nakai, K.; Kurahashi, T.; Matsubara, S. Nickel-Catalyzed Cycloaddition of *o*-Arylcarboxybenzonitriles and Alkynes via Cleavage of Two Carbon-Carbon σ Bonds. *J. Am. Chem. Soc.* **2011**, *133* (29), 11066–11068.
- (19) Minami, Y.; Yoshiyasu, H.; Nakao, Y.; Hiyama, T. Highly Chemoselective Carbon-Carbon σ -Bond Activation: Nickel/Lewis Acid Catalyzed Polyfluoroarylcyanation of Alkynes. *Angew. Chem., Int. Ed.* **2013**, *52* (3), 883–887.
- (20) (a) Xu, Z.-Y.; Zhang, S.-Q.; Liu, J.-R.; Chen, P.-P.; Li, X.; Yu, H.-Z.; Hong, X.; Fu, Y. Mechanism and Origins of Chemo- and Regioselectivities of Pd-Catalyzed Intermolecular σ -Bond Exchange between Benzocyclobutenones and Silacyclobutenes: A Computational Study. *Organometallics* **2018**, *37* (4), 592–602. (b) Li, X.; Hong, X. Computational Studies on Ni-Catalyzed C-O bond Activation of Esters. *J. Organomet. Chem.* **2018**, *864*, 68–80. (c) Ji, C.-L.; Hong, X. Factors Controlling the Reactivity and Chemo-selectivity of Resonance Destabilized Amides in Ni-Catalyzed Decarbonylative and Nondecarbonylative Suzuki-Miyaura Coupling. *J. Am. Chem. Soc.* **2017**, *139* (43), 15522–15529. (d) Ji, C.-L.; Hong, X. Factors Controlling the Reactivity and Chemoselectivity of Resonance Destabilized Amides in Ni-Catalyzed Decarbonylative and Nondecarbonylative Suzuki-Miyaura Coupling. *J. Am. Chem. Soc.* **2017**, *139* (43), 15522–15529.
- (21) (a) Guan, W.; Sakaki, S.; Kurahashi, T.; Matsubara, S. Reasons Two Nonstrained C-C σ -Bonds Can Be Easily Cleaved in Decyanative [4+2] Cycloaddition Catalyzed by Nickel(0)/Lewis Acid Systems. Theoretical Insight. *ACS Catal.* **2015**, *5* (1), 1–10. (b) Ni, S.-F.; Yang, T.-L.; Dang, L. Transfer Hydrocyanation by Nickel(0)/Lewis Acid Cooperative Catalysis, Mechanism Investigation, and Computational Prediction of Shuttle Catalysts. *Organometallics* **2017**, *36* (15), 2746–2754. (c) Zhu, B.; Du, G.-F.; Ren, H.; Yan, L.-K.; Guan, W.; Su, Z.-M. Synergistic Mechanistic Study of Nickel(0)/Lewis Acid Catalyzed Cyanoesterification: Effect of Lewis Acid. *Organometallics* **2017**, *36* (24), 4713–4720.
- (22) Guan, W.; Sakaki, S.; Kurahashi, T.; Matsubara, S. Theoretical Mechanistic Study of Novel Ni(0)-Catalyzed [6-2+2] Cycloaddition Reactions of Isatoic Anhydrides with Alkynes: Origin of Facile Decarboxylation. *Organometallics* **2013**, *32* (24), 7564–7574.
- (23) Zhao, Y.; Truhlar, D. G. The M06 Suite of Density Functionals for Main Group Thermochemistry, Thermochemical Kinetics, Noncovalent Interactions, Excited States, and Transition Elements: Two New Functionals and Systematic Testing of Four M06-Class Functionals and 12 Other Functionals. *Theor. Chem. Acc.* **2008**, *120* (1), 215–241.
- (24) Hay, P. J.; Wadt, W. R. Ab initio Effective Core Potentials for Molecular Calculations. Potentials for K to Au Including the Outermost Core Orbitals. *J. Chem. Phys.* **1985**, *82* (1), 299–310.
- (25) (a) Fukui, K. Formulation of the Reaction Coordinate. *J. Phys. Chem.* **1970**, *74* (23), 4161–4163. (b) Fukui, K. The Path of Chemical Reactions—the IRC Approach. In *Frontier Orbitals And Reaction Paths: Selected Papers of Kenichi Fukui*; World Scientific: Singapore, 1997; pp 471–476.
- (26) Mammen, M.; Shakhnovich, E. I.; Deutch, J. M.; Whitesides, G. M. Estimating the Entropic Cost of Self-Assembly of Multiparticle Hydrogen-Bonded Aggregates Based on the Cyanuric Acid-Melamine Lattice. *J. Org. Chem.* **1998**, *63* (12), 3821–3830.
- (27) The same methodology has been used in many theoretical studies: (a) Zeng, G.; Sakaki, S. Unexpected Electronic Process of H₂ Activation by a New Nickel Borane Complex: Comparison with the Usual Homolytic and Heterolytic Activations. *Inorg. Chem.* **2013**, *52* (6), 2844–2853. (b) Lu, Q.; Yu, H.; Fu, Y. Mechanistic Study of Chemoselectivity in Ni-Catalyzed Coupling Reactions between Azoles and Aryl Carboxylates. *J. Am. Chem. Soc.* **2014**, *136* (23), 8252–8260. (c) Jindal, G.; Sunoj, R. B. Importance of Ligand Exchanges in Pd(II)-Brønsted Acid Cooperative Catalytic Approach to Spirocyclic Rings. *J. Am. Chem. Soc.* **2014**, *136* (45), 15998–16008. (d) Dang, L.; Ni, S. F.; Hall, M. B.; Brothers, E. N. Uptake of One and Two Molecules of 1,3-Butadiene by Platinum Bis(dithiolene): A Theoretical Study. *Inorg. Chem.* **2014**, *53* (18), 9692–9702. (e) Jiang, Y.-Y.; Zhang, Q.; Yu, H.-Z.; Fu, Y. Mechanism of Aldehyde-Selective Wacker-Type Oxidation of Unbiased Alkenes with a Nitrite Co-Catalyst. *ACS Catal.* **2015**, *5* (3), 1414–1423. (f) Yin, G.; Kalvet, I.; Englert, U.; Schoenebeck, F. Fundamental Studies and Development of Nickel-Catalyzed Trifluoromethylthiolation of Aryl Chlorides: Active Catalytic Species and Key Roles of Ligand and Traceless MeCN Additive Revealed. *J. Am. Chem. Soc.* **2015**, *137* (12), 4164–4172. (g) Neufeldt, S. R.; Jiménez-Osés, G.; Huckins, J. R.; Thiel, O. R.; Houk, K. N. Pyridine N-Oxide vs Pyridine Substrates for Rh(III)-Catalyzed Oxidative C-H Bond Functionalization. *J. Am. Chem. Soc.* **2015**, *137* (31), 9843–9854.
- (28) Dolg, M.; Wedig, U.; Stoll, H.; Preuss, H. Energy-Adjusted Abinitio Pseudopotentials for the First Row Transition Elements. *J. Chem. Phys.* **1987**, *86* (2), 866–872.
- (29) (a) Barone, V.; Cossi, M. Quantum Calculation of Molecular Energies and Energy Gradients in Solution by a Conductor Solvent Model. *J. Phys. Chem. A* **1998**, *102* (11), 1995–2001. (b) Cossi, M.; Rega, N.; Scalmani, G.; Barone, V. Energies, Structures, and Electronic Properties of Molecules in Solution with the C-PCM Solvation Model. *J. Comput. Chem.* **2003**, *24* (6), 669–681. (c) Tomasi, J.; Mennucci, B.; Cammi, R. Quantum Mechanical Continuum Solvation Models. *Chem. Rev.* **2005**, *105* (8), 2999–3094.
- (30) Frisch, M. J.; Trucks, G. W.; Schlegel, H. B.; Scuseria, G. E.; Robb, M. A.; Cheeseman, J. R.; Scalmani, G.; Barone, V.; Mennucci, B.; Petersson, G. A.; Nakatsuji, H.; Caricato, M.; Li, X.; Hratchian, H. P.; Izmaylov, A. F.; Bloino, J.; Zheng, G.; Sonnenberg, J. L.; Hada, M.; Ehara, M.; Toyota, K.; Fukuda, R.; Hasegawa, J.; Ishida, M.; Nakajima, T.; Honda, Y.; Kitao, O.; Nakai, H.; Vreven, T.; Montgomery, J. A., Jr.; Peralta, J. E.; Ogliaro, F.; Bearpark, M.; Heyd, J. J.; Brothers, E.; Kudin, K. N.; Staroverov, V. N.; Kobayashi, R.; Normand, J.; Raghavachari, K.; Rendell, A.; Burant, J. C.; Iyengar, S. S.; Tomasi, J.; Cossi, M.; Rega, N.; Millam, J. M.; Klene, M.; Knox, J. E.; Cross, J. B.; Bakken, V.; Adamo, C.; Jaramillo, J.; Gomperts, R.; Stratmann, R. E.; Yazyev, O.; Austin, A. J.; Cammi, R.; Pomelli, C.; Ochterski, J. W.; Martin, R. L.; Morokuma, K.; Zakrzewski, V. G.; Voth, G. A.; Salvador, P.; Dannenberg, J. J.; Dapprich, S.; Daniels, A. D.; Farkas, Ö.; Foresman, J. B.; Ortiz, J. V.; Cioslowski, J.; Fox, D. J. *Gaussian 09*, Revision B.01; Gaussian, Inc.: Wallingford, CT, 2009.
- (31) Legault, C. Y. *CYLview*, 1.0b; Université de Sherbrooke: Sherbrooke, Quebec, Canada, 2009. <http://www.cylview.org>.
- (32) Zeng, G.; Sakaki, S. Noble Reaction Features of Bromoborane in Oxidative Addition of B-Br σ -Bond to [M(PMe₃)₂] (M = Pt or Pd): Theoretical Study. *Inorg. Chem.* **2011**, *50* (11), 5290–5297.
- (33) Ateşin, T. A.; Li, T.; Lachaize, S.; García, J. J.; Jones, W. D. Experimental and Theoretical Examination of C-CN Bond Activation of Benzonitrile Using Zerovalent Nickel. *Organometallics* **2008**, *27* (15), 3811–3817.
- (34) It is reasonable to speculate that such an active intermediate (2d) would be likely to react with stable intermediate 3a based on the “persistent radical effect”. Fischer, H. The Persistent Radical Effect: A Principle for Selective Radical Reactions and Living Radical Polymerizations. *Chem. Rev.* **2001**, *101* (12), 3581–3610.
- (35) (a) Lu, T.; Chen, F. Multiwfn: A Multifunctional Wavefunction Analyzer. *J. Comput. Chem.* **2012**, *33* (5), 580–592. (b) Xiao, M.; Lu, T. Generalized Charge Decomposition Analysis (GCDA) Method. *J. Adv. Phys. Chem.* **2015**, *04*, 111–124 (in Chinese).
- (36) Bickelhaupt, F. M.; Houk, K. N. Analyzing Reaction Rates with the Distortion/Interaction-Activation Strain Model. *Angew. Chem., Int. Ed.* **2017**, *56* (34), 10070–10086.